

## Article

# Precipitation of minerals from water-rich fumarolic gas using a flow-through benchtop installation

Michael Zelenski<sup>1\*</sup>, Yuri Taran<sup>2</sup>, Alina A.Korneeva<sup>1</sup>, Fedor D. Sandalov<sup>3</sup>, Nikolai Nekrylov<sup>1</sup>

<sup>1</sup> Institute of Experimental Mineralogy RAS, 143432, Chernogolovka, Russia; [volcangas@gmail.com](mailto:volcangas@gmail.com)

<sup>2</sup> Institute of Volcanology and Seismology FEB RAS, 683006, Petropavlovsk-Kamchatsky, Russia; [yuri.taran@gmail.com](mailto:yuri.taran@gmail.com)

<sup>3</sup> Faculty of Geology, Moscow State University, Vorobievsky Gory, 119991 Moscow, Russia; [fyodor.sandalov@yandex.ru](mailto:fyodor.sandalov@yandex.ru)

\* Correspondence: [volcangas@gmail.com](mailto:volcangas@gmail.com)

**Abstract:** Volcanic fumaroles are openings in the earth's surface, where volcanic gases discharge to the atmosphere. Metallic and non-metallic elements contained in gases form specific mineral precipitates upon cooling. Although the presence of metals in fumarolic gases has long been known, their concentrations are generally low and difficult to measure directly. A laboratory model of a fumarole may resolve the situation if the complex gas composition could be accurately reproduced. Here we describe a new experimental approach that allows accurately simulating fumarolic gases in terms of their main components (H<sub>2</sub>O, CO<sub>2</sub>, S, HCl), as well as adding volatile metal compounds. Gas is generated inside a special flow-through reactor, at the outlet of which the elements contained in the gas form temperature-dependent mineral sequence inside the attached silica-glass tube. Using this installation, we obtained laboratory sublimates from reducing (H<sub>2</sub>S-rich) gases similar to natural ones in terms of mineral composition and mineral habits. Twenty-one phases have been identified in sublimates, among which are simple and complex chlorides, simple sulfides and six sulfosalts. Comparison of the sublimate deposition from H<sub>2</sub>O-rich gas at 1 bar with similar works performed in evacuated ampoules at low pressure showed that fumarolic gases behave like an ideal gas, in which molecules do not interact with each other, and reactive compounds in the gas serve in fact as an inert carrier of volatile metals species. Changing the composition of the gas at the outlet of the installation, its flow rate and temperature, we can observe the corresponding changes in mineral precipitates and in such a way study the factors affecting mineral formation on natural fumarolic fields.

**Keywords:** benchtop fumarole, flow-through reactor, sublimates, volatile metal species, simulation

## 1. Introduction

Volcanic fumaroles attract attention as an accessible place where volcanic gases, which carry information from the Earth interior, can be studied [e.g., reviews by [1](#), [2](#), [3](#), [4](#), and references therein]. Fumaroles are present on erupting or persistently degassing volcanoes, and look like as holes or areas on the ground where volcanic gas discharges to the atmosphere. Such sites are typically covered with altered rocks and multi-colored deposits called "fumarolic incrustations" and "fumarolic sublimates" [e.g., [5](#), [6-8](#)]. In terms of mineral and chemical composition, fumarolic deposits differ significantly from the surrounding rocks, which is explained by hydrothermal alteration of rocks under the influence of acid gases [[6](#), [9](#)], as well as by the precipitation of elements transported by gases [e.g., [10](#), [11](#)]. Strictly speaking, the term "sublimates" is not correct. From a physical point of view, "sublimation" is evaporation without melting, and the reverse process, including that observed on volcanoes, should be called "desublimation". Terminology

that is used in chemistry calls these processes as “chemical vapor deposition”. However, the term “sublimates” is widely used in volcanological literature and will be used below.

It has long been known that volcanic (fumarolic) gases can transport significant amounts of metals. Back in the 19th and early 20th centuries, numerous researchers (T. Monticelli, P. Kremers, F. Zambonini, G. Carrobbi, A. Lacroix) of Italian volcano Vesuvius, known for its diverse mineralogy, explained the presence of incrustations around fumaroles by the deposition of metals from the gas [12]. The Valley of Ten Thousand Smokes in Alaska, formed after the eruption of Katmai volcano in 1912, is considered a classic example of the deposition of heavy metal sulfides from fumarolic gases [13, 14]. The possible role of volcanic gas transport of elements in the genesis of ore deposits was also discussed in detail [15, 16].

Sublimates are enriched in elements having volatile (high vapor pressure) compounds [e.g., 7, 17, 18]. The most common are metallic elements Cu, Cd, Pb, Bi, Tl, followed by V, In, Mo, W, Re and Au. Of the rock-forming elements, compounds of Na, K and Fe are often present in sublimates. Non-metals almost always present are S, Se, Te, F, Cl, Br and I, As and B, as well as NH<sub>3</sub>. The listed elements (in the case of reduced gases, i.e., not diluted with air) form sulfides, sulfosalts, halides, oxides, and also precipitate in the form of native elements. Sulfur is most abundant among the latter, but native metals such as gold are also common on some volcanoes [19, 20]. A well-studied site with a plentiful reduced mineral precipitates is the crater La Fossa on Vulcano Island, Italy [21]. Volcanoes Kudryavy (Kurile Islands), Mutnovsky (Kamchatka) and Merapi (Indonesia) are also good examples of the reduced fumarole-related mineral deposition [18, 22, 23].

The listed compositional features are characteristic of fumaroles with reduced gas composition. The composition of sublimates critically depends on  $fO_2$  ( $fH_2$ ) in the gas, and sublimates in the oxidized fumaroles (i.e., where mixing of initially reduced gases with atmospheric air has occurred) are completely different. Oxidized sublimates often develop in cracks above lava flows and on cooling cinder cones of recent eruptions. The oxidized fumaroles are characterized by mineral associations consisting of sulfates, selenates, arsenates, vanadates, molybdates of Na, K, Fe, Cu, Zn and other elements. Typical oxidized fumaroles are located on the summit of Colima volcano (Mexico) [17] and on cooling eruptive cones after the 1975 Tolbachik volcano (Kamchatka), where an exceptional mineral diversity is observed [24].

In addition to numerous mineralogical studies on natural fumarolic fields, some experimental works were made in order to clarify questions that could not be solved by studying natural samples. The first known is a method of “silica glass tube”, applied by [Le Guern, F. and Bernard, A. \[25\]](#) on Mount Merapi. In a silica glass tube inserted into a fumarolic vent, elements precipitate from gradually cooling supersaturated gas as the latter moves from the vent to the tube outlet. The collected “sublimates” are typically zoned and can be further studied for their element and phase composition. The method suggested by [Le Guern, F. and Bernard, A. \[25\]](#) makes it possible to study the growth of minerals from the gas phase in natural environment. The method also allows revealing the presence of the most rare elements in the gas (Re, Os, Ir, Pt) due to the high degree of the element concentration during their deposition from the gas onto the walls of the silica tube [26]. Several recent works in the laboratory have experimentally studied volatilization of elements from silicate melt (or solid oxides), in the presence or absence of ligand-forming non-metals (sulfur, chlorine), followed by gaseous transport and deposition onto tube walls as “sublimates” (strictly saying, precipitates in the tube formed due to desublimation process). [Nekvasil, H. et al. \[27\]](#) and [Renggli, C.J. and Klemme, S. \[28\]](#) used evacuated ampoules for the study, whereas Scholtysik and Canil [29–31] worked at atmospheric pressure, using gaseous atmosphere with different  $fO_2$ .

The ultimate goal of all such experiments is to identify factors and laws that determine the trace element composition of fumarolic gases and the conditions of transport of metals and metalloids with volcanic and fumarolic gases and deposition of minerals from such gases. This is where the laboratory experiments are necessary. Although the results of such experiments with “benchmark fumaroles” are interesting, they do not represent a

fully-featured model of a natural fumarole. The main shortcoming of the experimental approaches described above is that they do not contain water in the model gas composition. At the same time, water steam is the main gas component in natural volcanic fumaroles. Therefore, hydrogen makes 2/3 of the fumarolic gas, counting atomic %. This means that in a laboratory experimental model “fumarole” without water, trace elements cannot be transported as gaseous hydrates, hydrides, hydroxides and other hydrogen-containing compounds, while the listed species are abundant in natural fumarolic gases [e.g., 7, 9, 23, 32, 33]. The mentioned studies simulate gaseous transport of elements only for some very special conditions such as low-pressure gas transport on Mars [27], or the degassing of anhydrous silicate melts that are rare in natural environment (Scholtysik and Canil [29-31]). The common volcanic fumaroles and gaseous transport in water- and hydrogen-rich medium as well as the element deposition from such gas differ significantly from the installations that use evacuated vials or evaporation from a silicate melt.

Two goals of this work were formulated as follows: (1) to obtain reproducible mineral precipitates (sublimates) of a certain composition, closely matching the sublimates on natural volcanoes; and (2) these sublimates should be obtained from a gas coinciding with natural fumarolic gases in terms of major gas species. Below we present a new experimental method for modeling of the gaseous transport of elements and mineral deposition, which is able to replicate natural conditions on a fumarolic field, providing the element precipitation from water-rich high-temperature gas containing HCl and sulfur. Our experimental setup consists of two parts (combined into one installation), which sequentially performed two tasks: (1) to provide a stable gas flux containing  $\text{H}_2\text{O-S-HCl} \pm \text{CO}_2$  and generally resembling natural fumarolic gases; and (2) to add VMS (Volatile Metal and metalloid Species) as well in order to obtain sublimates closely matching the natural (fumarolic) sublimates. The method can be useful in simulation of trace element transport and mineral deposition in natural fumaroles for a wide range of gas compositions, including reduced and oxidized fumarolic gases. Using a thermochemical code we estimated the equilibrium composition of the resulting gas phase mixture along the temperature gradient and described mineral precipitates in the silica glass tube, attached to the artificial “fumarole”. Detailed presentation of the gas composition data and corresponding discussion will be published elsewhere.

## 2. Experimental technique and setup design

### 2.1. Experimental setup

The experimental setup consists of a main gas generator ( $\text{H}_2\text{O-CO}_2\text{-SO}_2\text{-H}_2\text{S-HCl}$ ) and a trace element generator (e.g., Na, K, Fe, Cu, Zn, As, Cd, Pb, Tl, Bi, Br and I), both parts being combined inside one casing. At least one attempt is known from literature to simulate the composition of fumarolic gas using gases from commercially available cylinders. Mioduszewski, L. and Kress, V. [34] in their “artificial laboratory fumarole” added sulfur in the form of gaseous  $\text{SO}_2$  from a cylinder and additional hydrogen ( $\text{H}_2$ ) from another cylinder in order to reduce some  $\text{SO}_2$  to  $\text{H}_2\text{S}$ . However, the technology with cylinders filled with toxic or flammable gases seems to be complex and unsafe. The kinetics of  $\text{SO}_2$  reduction with hydrogen (gas equilibration time) also raises questions. The reaction of  $\text{SO}_2$  reduction is relatively slow and require catalysts, even at temperatures of 800-1000 °C [e.g., 35, and references therein]. We considered that such a technology is complicated, inconvenient, and does not accurately reproduce the composition of the gas under study. It was also taken into account that small liquid flows (of the order of 1-10  $\text{mm}^3/\text{s}$ ) are much easier to create from the technical point of view than a small stable flow (approximately 1-10  $\text{cm}^3/\text{s}$ ) of a gas having a complex and aggressive composition. The simplified volcanic gas (without fluorine and trace elements) is described by the H-C-O-S-Cl system of elements, which corresponds to the system  $\text{H}_2\text{O-H}_2\text{-CO}_2\text{-CO-SO}_2\text{-H}_2\text{S-HCl}$  of gas species. To simulate such a gas system, we used the evaporation of two liquids. The liquid #1 ( $\text{H}_2\text{O} + \text{H}_2\text{O}_2 + \text{HCl}$ ) contains water, hydrogen

chloride, and excess oxygen in the form of hydrogen peroxide ( $\text{H}_2\text{O}_2$ ) to adjust the required redox state of the gas. The role of the liquid #2 (carbon disulfide,  $\text{CS}_2$ ) was to supply sulfur to the system.

The installation design is shown in Figures 1 and 2. Peristaltic pumps #1 and #2 deliver liquids #1 and #2 to the evaporator. Each pump is equipped with a pulse dampener to eliminate pulsations. The dampener was made using a piece of Viton tubing of 1.6 mm I.D., coupled with a glass capillary (Figure 2). The Viton tubing section in this case serves as a retaining vessel of the dampener. To control the liquid supply rate, drip chambers were installed after each pulse dampener. Such control is necessary because of the possible instability of the fluid supply rate due to swelling, or vice versa, stretching of the tube in the peristaltic pump. The drip chambers were made of plastic medical syringes, with Teflon capillary tube inserted through a silicone rubber stopper. This allowed us measuring flow rate of the liquids by counting drops in a time interval. Before each experiment, we calibrated the pumps and compared the calibration value of the liquid flow rate to the drip chambers counts. Drip chambers are widely used in clinical practice for drug administration. Drop size in the drip chamber varies with liquid composition, drip orifice diameter and shape but remains stable for a given drip chamber and for the same liquid [e.g., 36].

For pumping aggressive liquids (carbon disulfide), we used fluoroelastomer tubing (Viton / Fluran 5050) with an inner diameter of 1.02 or 1.6 mm, and connecting PTFE tubing (Figure 2). Further, the liquid flows through PTFE capillary tubing into an evaporator made of silica fiber, placed into a silica glass tube (Figure 3). The evaporator is located in the zone of an ascending temperature gradient from ambient ( $\sim 20^\circ\text{C}$ ) to  $> 150^\circ\text{C}$ , when all components are known to pass into a gaseous state. After evaporation of liquids and heating of vapors to approximately  $900^\circ\text{C}$ , the gas mixture enters a flow-through tubular reactor made of silica glass. The reactor is filled with 2-3 mm fraction granules of finely porous sintered corundum ( $\text{Al}_2\text{O}_3$ ), which plays mainly the role of inert filler, but also as a catalyst for  $\text{CS}_2$  hydrolysis [37]. The temperature in the reactor during the described experiments was maintained at  $900^\circ\text{C}$ , but can be increased up to  $1250^\circ\text{C}$ . The optimal gas flux (i.e., having such a velocity that would allow complete reactions between the main volatile components and deposition of sublimates from the gas phase) was selected empirically and amounted to  $\sim 1$  g/min ( $\sim 16.7$  mg/s). This corresponds to approximately 4.8 l/min (80 ml/s) of the gas at  $900^\circ\text{C}$ . With experiment duration of 8 hours, about 0.5 kg of gas is pumped through the installation, which at an operating temperature of  $\sim 900^\circ\text{C}$  makes about  $2.4\text{ m}^3$  of the gas.

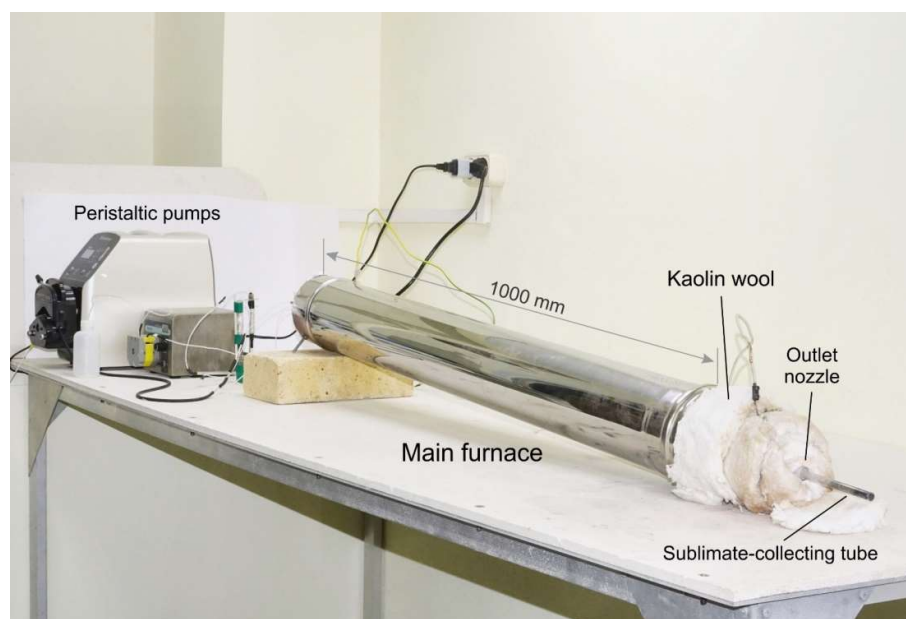


**Figure 1.** General view of the experimental setup for modeling fumarolic mineral formation. A part of the furnace shell has been removed to show the thermal insulation (kaolin wool) and the outlet nozzle of the tubular reactor. The feeding system of the reactor is shown in detail in Figure 2; the internal structure of the reactor is shown in Figure 3.

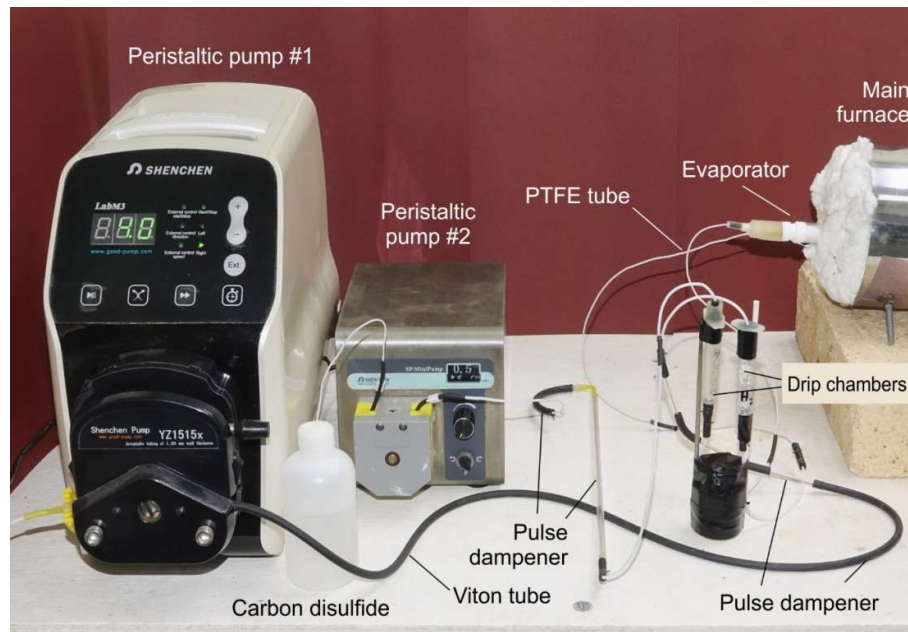


**Figure 2.** The feeding system for major gas species of the experimental installation consists of two peristaltic pumps that pump two liquids (water solution of  $\text{HCl} + \text{H}_2\text{O}_2$  and carbon disulfide) to the reactor evaporator. The system is equipped with pulse dampeners to eliminate flow pulsations and drip chambers to keep a check on volume flow rate.

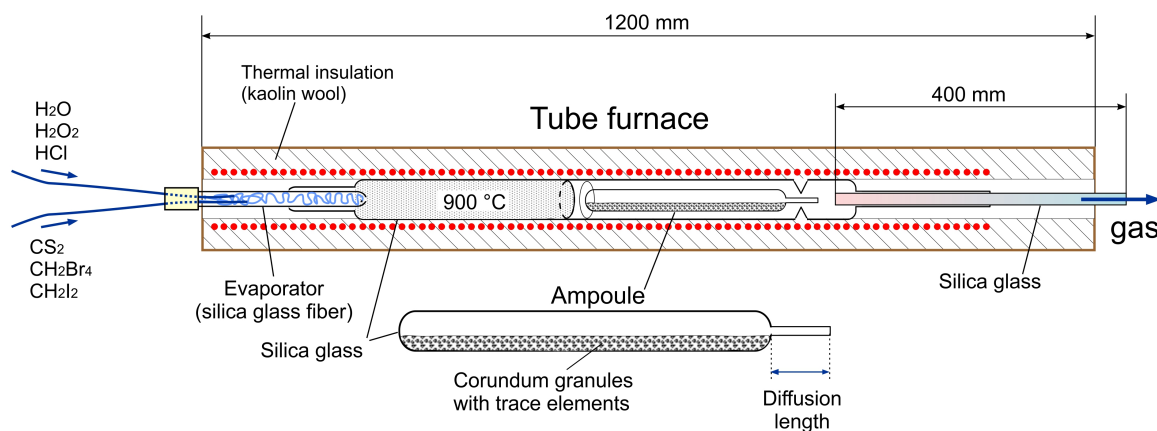


**Figure 3.** The internal structure of the reactor shown in Figure 1. The reactor is located in a silica glass tube furnace, thermally insulated with kaolin wool. The furnace temperature is regulated by a thermocouple (not shown in the Figure). Inside the furnace are the evaporator and the reactor itself, filled with corundum granules. All component of the reactor, except corundum granules, are made of silica glass. In the right part of the reactor is located an ampoule filled with corundum granules supplying VMS to the gas. The granules inside this ampoule are covered with metal oxides and salts (see Fig. 4). The



inner space of the ampoule is connected with the surrounding atmosphere via a short tube, where diffusion of the gas components takes place. The gas leaves the reactor through a silica glass tube in the temperature gradient zone, where sublimates are deposited.

2.2. Carbon disulfide as a source of sulfur in the experiment

The use of cylinder gases to simulate fumarolic gas [34] is inconvenient and involves technical and logistical challenges. We used carbon disulfide as a convenient substance for sulfur introducing into the simulated fumarolic gas. Carbon disulfide (CS<sub>2</sub>) is a volatile liquid (boils at 46.3 °C) that can be pumped using a damped peristaltic pump. The peristaltic pump creates a small fluid flow of the order of 1 mm<sup>3</sup>/s, and the damper eliminates the pulsations. Although carbon disulfide is a poisonous and fire hazardous liquid, these disadvantages can be compensated for by careful handling of this substance.

Hydrolysis reaction of CS<sub>2</sub> is widely used in industry. Already at a temperature of 50-70 °C, carbon disulfide is hydrolyzed in the presence of a catalyst [38], and at 400 °C, CS<sub>2</sub> rapidly reacts with water according to the reaction CS<sub>2</sub> + 2H<sub>2</sub>O = CO<sub>2</sub> + 2H<sub>2</sub>S [39, 40]. Further, hydrogen sulfide (H<sub>2</sub>S) is oxidized by oxygen, which is available in the system after decomposition of hydrogen peroxide at 150 °C (H<sub>2</sub>O<sub>2</sub> = H<sub>2</sub>O + 1/2 O<sub>2</sub>; 2H<sub>2</sub>S + 3O<sub>2</sub> = 2H<sub>2</sub>O + 2SO<sub>2</sub>). Oxidation of H<sub>2</sub>S has sufficiently fast kinetics [41] to comply with our requirements. The released CO<sub>2</sub> is an intrinsic component of fumarolic gases. Since the gases of volcanic fumaroles usually contain SO<sub>2</sub> and H<sub>2</sub>S simultaneously in a ratio close to 2:1 to 1:1 [42], some portion of H<sub>2</sub>S must be oxidized. We found that the most convenient way to perform partial oxidation of H<sub>2</sub>S was by adding a required amount of hydrogen peroxide (H<sub>2</sub>O<sub>2</sub>) to the hydrochloric acid solution. H<sub>2</sub>O<sub>2</sub> decomposes into water and oxygen above 150 °C, then the released oxygen oxidizes H<sub>2</sub>S to sulfur dioxide: 3H<sub>2</sub>O<sub>2</sub> = 3H<sub>2</sub>O + 3/2O<sub>2</sub>; H<sub>2</sub>S + 3/2O<sub>2</sub> = SO<sub>2</sub> + H<sub>2</sub>O. In such way, sulfur compounds were added to the gas flux. Literature data on the kinetics of the listed reactions at temperatures of the order of 900 °C are almost absent. However, based on kinetics at low temperatures, it can be expected that all the components in the H-C-O-S system will react with each other at a gas temperature of 900 °C in a time not exceeding the residence time, which for the selected reactor size is about 2 s.

2.3. Calculation of the gas composition

We calculated the composition and flow rates of the liquids supplied to the reactor inlet (evaporator) iteratively, based on the required composition of the experimental gas. The gas composition was calculated using thermodynamic calculations (HSC 6.1 software, Roine, A. [43]) based on a rough preliminary estimate of the composition and flow rate of the liquids supplied to the reactor (CS<sub>2</sub>, H<sub>2</sub>O<sub>2</sub>, etc.). Subsequently, the compositions and flow rates of liquids were refined using the results of thermodynamic modeling. For the experiments with the most common (reduced) fumarolic gas compositions, the calculations were performed under the assumption that the ratio of SO<sub>2</sub>: H<sub>2</sub>S in the model gas should be close to 2:1 at 900 °C. The calculations took into account the gas flow rate, the composition of the pumped liquids and their specific gravity. Without thermodynamic modeling, amounts of the initial liquids and compositions of the resulting gas can be hardly calculated. Table 1 shows the typical compositions and flow rates of the liquids supplied to the evaporator.

Table 1. Compositions, densities and supply rates for the pumped liquids.

Liquids	Components	Liquid flow rate, mm <sup>3</sup> /s	Liquid SG, mg/mm <sup>3</sup>	Component supply rate, 10 <sup>-6</sup> mol/s
---------	------------	--------------------------------------	-------------------------------	---

Liquid #1		15.6	1.056
H <sub>2</sub> O <sub>2</sub> , 60%	100 ml		68.36
HCl, 38%	20 ml		7.73
H <sub>2</sub> O	up to 500 ml		770.33
Liquid #2		1.21	1.26
CS <sub>2</sub>	60 ml		20.08
CH <sub>2</sub> I <sub>2</sub>	0.04 ml		0.0100
CH <sub>2</sub> Br <sub>4</sub>	0.1 ml		0.0174

#### 2.4. Trace elements in the model gas

Adding trace elements to experimental fumarolic gas (high-temperature and aggressive) is a technically challenging task. In several earlier works on modeling fumaroles, the element concentrations in the gas were under control of the element diffusion in silicate melt [29-31] or volatilization from metal oxides [28]. In both cases, the concentrations of elements in the gas were not appointed or measured. An opposite example is a well-known ICP-MS nebulizer, which creates a calibrated flux of trace elements in high temperature gas. For our simple experiment, we did not consider the possibility of using an expensive nebulizer or similar equipment. Alternatively, we applied a compromise solution by using a simple device without moving parts, which was capable of creating and maintaining relatively stable concentrations of a number of trace elements in the complex and aggressive gas mixture. As a parameter, which had to be neglected, the ability to arbitrarily set certain concentrations of elements was chosen.

The following procedure was used to add trace elements (Na, K, Fe, As, Cd, Pb, Tl, Bi, Br, I) to the gas. On the surface of corundum granules, metal compounds were deposited in the form of oxides (Fe, Cu, Cd, In, Tl, Pb, Bi), chlorides (Na, K), and arsenates (Na<sub>3</sub>AsO<sub>4</sub>). The process of preparing corundum granules is shown in the flowchart (Figure 4). Granules of porous sintered corundum (fraction 2–3 mm) were soaked in two separate solutions containing the assigned trace elements (Table 2). The solutions were prepared by mixing the corresponding components with gentle heating (50–60 °C). Then the granules were dried at 120 °C, and those with metal nitrates were exposed to two-step thermal decomposition at 300 and 700 °C. The second step at 700 °C was necessary to ensure the completeness of nitrate decomposition, as some nitrates (BiO(NO<sub>3</sub>)) may be still stable at 300 °C. Arsenate/chloride and nitrate solutions were used separately because precipitation occurs upon their mixing. Porous corundum was used as a convenient inert support that does not react at the temperature of the experiment (900 °C) with gases containing HCl and volatile sulfur compounds. The amounts of the components (Table 2) for the preparation of solutions #1 and #2 were not specially calculated in this work, and were chosen somewhat arbitrarily.

**Table 2.** Components for the preparation of solutions.

Component	Weight, g		
	Run #1	Run #2	Run #3
Solution #1			
NaCl	2.060	4.290	2.150
KCl		4.120	2.290

Na <sub>3</sub> AsO <sub>4</sub> ·12H <sub>2</sub> O	0.472	0.320	0.402
H <sub>2</sub> O	50 ml	50 ml	50 ml
Solution #2			
TiCl <sub>3</sub>	0.635	0.671	0.774
Bi <sub>2</sub> O <sub>3</sub>	1.150	0.546	0.850
CuO		0.582	
In (metal)			0.260
Fe(NO <sub>3</sub> ) <sub>3</sub> ·9H <sub>2</sub> O	2.340	1.023	2.120
Pb(NO <sub>3</sub> ) <sub>2</sub>	0.950	0.605	0.857
Cd(NO <sub>3</sub> ) <sub>2</sub> ·4H <sub>2</sub> O	1.060	0.737	0.886
HNO <sub>3</sub> (63%)	50 ml	50 ml	50 ml

After preparation of corundum granules, these granules were put into a silica glass ampoule of a special shape (Figure 5) so as to fill approximately 1/3 of the ampoule volume. The inner volume of the ampoule is connected with the external environment through a short “diffusion tube”. Because the inner diameter of the ampoule is several times larger than the diameter of the diffusion tube, the diffusion flux of elements out from the ampoule into the created gas flow is mainly controlled by diffusion through the narrow diffusion tube.

When the experimental setup is in operation, gas with the operating temperature 900 °C diffuses through the diffusion tube into the ampoule filled with corundum granules coated with metals oxides and salts. Inside the ampoule, gas reacts with the components deposited on the corundum surface (metal oxides, chlorides and arsenates). The resulting volatile metal species diffuse through the tube in the opposite direction and mix with the gas flow inside the reactor (Figures 3, 5). The role of corundum grains is to evenly distribute metals in the volume of the ampoule and to facilitate gas access to the layers below the filling surface (granules similar in shape to spheres of equal size fill about 75% of the volume).

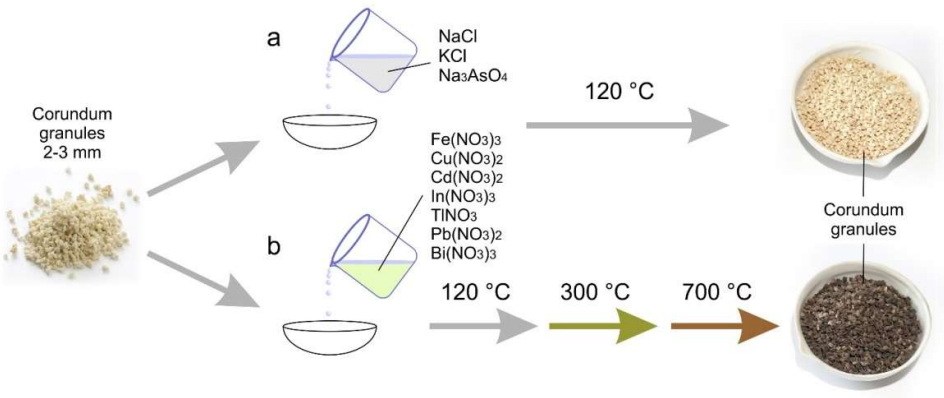


**Figure 4.** Flowchart showing the process of preparing corundum granules coated with metal salts (A) and oxides (B), which are then used to introduce volatile metal species (VMS) into the experimental gas.

We also added small amounts of bromine and iodine to the gas by mixing corresponding amounts of methylene iodide CH<sub>2</sub>I<sub>2</sub> and tetrabromoethane C<sub>2</sub>H<sub>2</sub>Br<sub>4</sub> to carbon



disulfide (Table 1). The described technique makes it possible to obtain a gas flow with known concentrations of the main components, and approximately constant (although unknown) concentrations of trace elements. The presence of the trace elements in the gas is confirmed by the deposition of mineral phases in the silica glass tube at the outlet nozzle of the experimental installation. To confirm the fact that the concentrations of trace elements in the gas changed relatively weakly during the experiment, we judged from comparison the patterns of sublimates sequentially deposited in 2-3 silica tubes, replaced one with another.

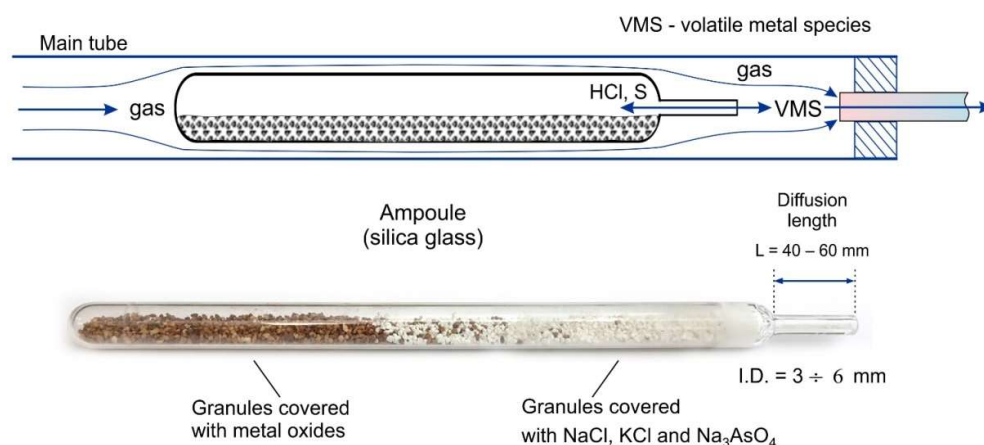


**Figure 5.** Feeding ampoule for introducing VMS to the experimental gas, and a scheme of the reactor with the ampoule. Granules covered with oxides (brown) and with salts (light) are shown in different parts of the ampoule for clarity. In a real experiment, the granules were thoroughly mixed.

### 2.5. The selenium and tellurium problem.

Selenium and tellurium are elements, which are abundant in natural fumarolic gases and sublimates [e.g., 18]. It was found, however, that Se and Te tend to volatilize from any compounds at lower temperature (200-600 °C) than almost all other elements. We have tried to add  $\text{TeO}_2$ , sodium tellurate and selenate ( $\text{Na}_2\text{TeO}_4$  and  $\text{Na}_2\text{SeO}_4$ ), and iron telluride and selenide ( $\text{FeTe}$ ,  $\text{FeSe}$ ) as a source compound. As a consequence, the concentrations of Se and Te in the gas were excessively high at the beginning of the experiment, but then rapidly decreased, while the concentrations of the remaining elements were relatively stable. For this reason, we have excluded selenium and tellurium from the list of elements for modeling until the problem is solved.

### 2.6. Experimental conditions and technique

All experiments with the deposition of sublimates were carried out under approximately the same conditions: reactor temperature 900 °C, composition and flow rate of feeding liquids as in Table 1, duration of sublimite deposition 2-6 hours. In each of the experiments, the ampoule for VMS introduction was prepared in accordance with Table 2 and flowchart from Figure 4. The assembled installation was heated to an operating temperature of 900 °C and then the pumps were switched on. Approximately 10-15 minutes after the start of the liquid supply, a silica glass tube 10x8x400 mm (O.D.-I.D.-L.) was inserted into the outlet nozzle, in which the sublimates further precipitated. The required temperature gradient in the range of 900-120 °C appeared in the tube both due to the temperature field of the main heater (conductive heat transfer) and convective heat

transfer with the gas flow. The thickness of the heat insulation at the outlet of the reactor was adjusted so that the gas temperature at the very end of the tube with sublimates remained slightly above 100 °C in order to avoid condensation of water. After the end of the experiment, a silicone hose was put on the cold end of the tube, through which a weak flow of argon was passed; after that, the tube with sublimates was removed. This made it possible to avoid the oxidation of small crystals of sublimates by atmospheric oxygen. During some experiments, several tubes were replaced sequentially in order to reveal changes in the elemental composition of the gas.

### 3. Sampling and analysis

#### 3.1. Gas sampling.

Gas sampling was carried out to check up the recovery of elements (S, Cl), which are supplied to the reactor inlet. The sampling was carried out using a standard “Giggenbach bottle” as well as with a syringe and a ceramic capillary. The standard “Giggenbach bottle” is a borosilicate glass ampoule with a PTFE stopcock and is routinely used for gas sampling on active volcanoes [44]. The gas flow rate at the outlet of the installation (~ 27 ml/s at 120 °C) allows using a “Giggenbach bottle” (Figure 6). However we found, that a more convenient way of sampling was to collect gas into a plastic medical syringe through a ceramic capillary (Figure 7). Approximately 10 ml of 4N KOH solution was put into the syringe before sampling. The syringe was weighed before and after sampling, the weight gain was determined by the difference. Typically, samples were taken with a weight gain of about 1 g. For H<sub>2</sub>S analyses, gas condensation was applied into the 1N Cd(NO<sub>3</sub>)<sub>2</sub> solution.

To determine the total sulfur and chlorine in the samples, we used the method adopted for natural volcanic gases [44]. The samples were oxidized with H<sub>2</sub>O<sub>2</sub>, then diluted to 40 ml. Chloride was determined by titration in neutral solution according to Mohr. Total sulfur as sulfate was analyzed using turbidimetric method. Samples for H<sub>2</sub>S were analyzed gravimetrically by weighing the CdS precipitate, dried at 110 °C. For each point of the gas composition, three samples were taken, which were then averaged.

#### 3.2. Processing and analyzing of sublimates.

The silica glass tubes with the precipitated sublimates were split into small fragments of approximately 1 cm in size in such a way as to preserve the temperature sequence, i.e. without displacement of fragments. The fragments were glued to glass specimen holders and photographed in reflected light (Nikon Eclipse LV100N-POL Microscope). Further, the fragments of the tube were studied under a scanning electron microscope with local energy-dispersive X-ray microanalysis (SEM-EDS, Vega Tescan II XMU, IEM RAS, Chernogolovka). An accelerating voltage of 15–20 kV and a probe current of 300–400 pA were applied for analyses. For unpolished samples, the accuracy of the EDS analysis depends on the surface angle of a specimen. For such samples, we used a method described, for example, in [45]. In each of the analyzes, we tried to find relatively horizontal regions on the sample and repeated analyzes to obtain averages, or rotated the specimen by 180 ° and averaged two analyzes taken before and after rotation. Many analyzed samples, especially from the hottest part of the tube, showed excessive oxygen content presumably to partial oxidation of tiny crystals after pulling out the tube from the installation. For such cases, crystal morphology characteristic of the supposed minerals was taken into account.



**Figure 6.** Sampling the total gas sampling using “Giggenbach bottle”. A – Gas escape from the cold end of the sublimate-collection tube; yellow deposits of sulfur are visible. B – Gas sampling via a ceramic capillary into 4N KOH solution.



**Figure 7.**  $\text{H}_2\text{S}$  sampling into 1N  $\text{Cd}(\text{NO}_3)_2$  solution using a plastic medical syringe through a ceramic capillary.

### 3. Results

#### 4.1. Main gas components

The resulting composition of the main components of the gas phase and corresponding discussion will be published elsewhere. Here we estimate concentrations of the main gas components in the temperature range 100 – 1200 °C, using thermodynamic modeling (HSC 6.1 program). Results are shown in Figure 8. At a temperature of 900 °C, the calculated ratio of the concentrations of sulfur dioxide and hydrogen sulfide ( $\text{SO}_2/\text{H}_2\text{S}$ ) is close to 2:1. With a decrease in temperature, the proportion of hydrogen sulfide first increases and then decreases to zero. Instead of hydrogen sulfide, elemental sulfur appears in the form of a fine aerosol of liquid sulfur droplets. Above 500 °C, a noticeable amount of molecular hydrogen appears, which is formed as a result of the "gas buffer" reaction [42]:  $\text{H}_2\text{S} + 2\text{H}_2\text{O} = \text{SO}_2 + 3\text{H}_2$ . At temperatures above 800 °C, carbon monoxide (CO) can be detected. The HCl concentration is stable over the entire temperature range.

The precipitation of the native sulfur at the cold end of the silica tube and a significant amount of the forming  $\text{H}_2\text{S}$  are shown in Figure 6a and Figure 7, which by some way supports the calculated equilibrium compositions. The redox potential and relative concentration of  $\text{H}_2$  in the H-C-O-S system can also be described in terms of mineral buffers in the RH vs. reciprocal temperature (Figure 9).

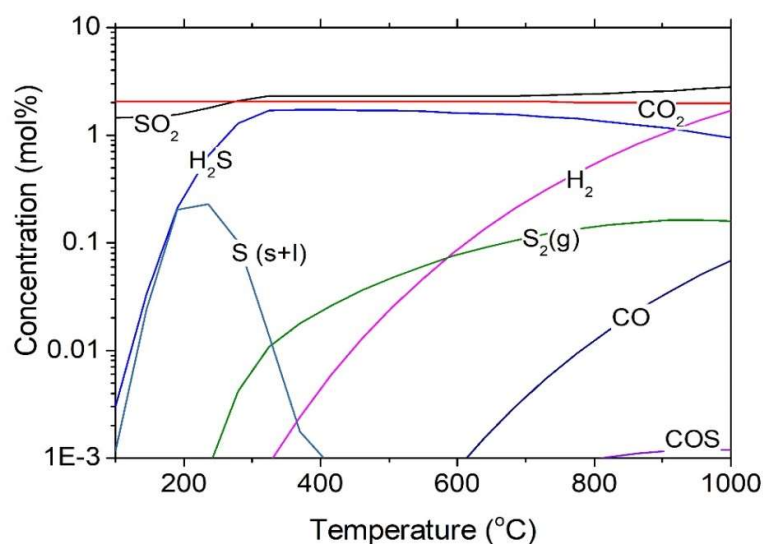


**Figure 8.** Calculated equilibrium concentrations of the main gas components in the temperature range 100 – 1200 °C with the initial composition (in mmol/mol):  $\text{H}_2\text{O}$  - 770.3;  $\text{H}_2\text{O}_2$  - 68.4;  $\text{HCl}$  - 7.73;  $\text{CS}_2$  - 20.1, Table 1).

To verify the ability of the experimental setup to generate gas close in its composition to natural fumarolic gases, we measured the sulfur concentration (as total S) and hydrogen chloride (HCl) concentration in the gas at the reactor outlet, depending on the supply rate of carbon disulfide (liquid # 2) to the reactor inlet, and with the constant supply rate of liquid #1. The verification results are present as input/output ratios (%) of the components (Figure 10). The presence of hydrogen sulfide in the gas at the outlet of the reactor was examined by precipitation of  $\text{CdS}$  during gas sampling into the 1N  $\text{Cd}(\text{NO}_3)_2$  solution (Figure 7). However, due to the rapid decrease in the concentration of hydrogen sulfide in the temperature gradient zone and the presence of elemental sulfur aerosol in the gas below 300 °C (Figure 8), the  $\text{H}_2\text{S}$  concentrations measured at the reactor

outlet most likely do not show exactly the equilibrium concentrations for any temperature.

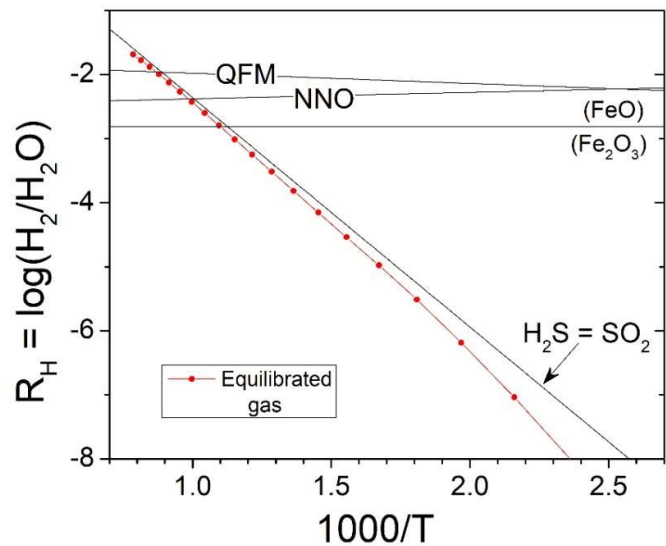


**Figure 9.** Redox diagram for volcanic gases in terms of  $R_H$  vs  $1000/T^{\circ}K$  [42]. Green line corresponds to the calculated  $R_H$  using code HSC 6.1 for the modeled gas with the initial composition (in mmol/mol)  $H_2O$  -770.3;  $H_2O_2$  - 68.4;  $HCl$  - 7.73;  $CS_2$  - 20.1). Standard redox solid buffers are also shown.

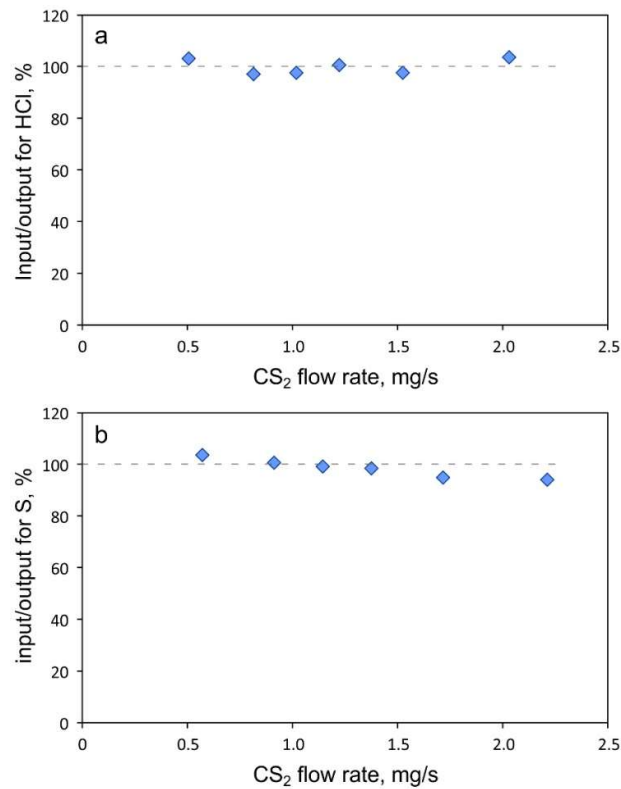


**Figure 10.** Measured input/output ratios for the total S and HCl in the experimental installation, depending on the supply rate of carbon disulfide at the reactor inlet.



### 3.2. Experimental sublimates in silica glass tubes

The main goal of the experiments was to obtain man-made (laboratory) sublimates in a silica glass tube, which reproduce the natural sequence of sublimates observed in fumarolic fields as closely as possible. This goal was achieved: we were able to carry out three successful experiments with reduced model gases (with a high content of hydrogen sulfide) and obtained temperature sequences of precipitates in silica glass tubes, which were similar to natural sublimates in their mineral composition. In each of the experiments, we slightly changed the composition of the solutions prepared for charging the feeding ampoule (Table 1, Figures 4, 5). The summary phase sequence versus temperature (combined from three experiments) is present in Figure 11; visual appearance of silica glass tubes after the experiment and fragments of tubes with sublimates, attached to glass specimen holders, are shown in Figure 12. Electron micrographs (back-scattered electron images, BSE) of individual phases are displayed in Figures 13-16.

The temperature sequence of the phases in experimental sublimates is similar to the sequence observed in silica glass tubes with sublimates, collected from natural fumarolic gases on Mutnovsky volcano [18]. Similar to the sublimates of Mutnovsky volcano, high-temperature simple sulfides are followed by high-temperature simple chlorides, then by complex sulfides (sulfosalts), complex halides of chalcophile elements, sulfur with arsenic (arsensulfurite), and elemental sulfur at the very end of the tube. Twenty-one phases were identified among the experimental sublimates, including seven halides, five simple sulfides and six sulfosalts. The lowest-temperature phases in the experiment, as well as in natural sublimates, were arsenous sulfur and elemental sulfur without arsenic. Experimental sublimates are different in their temperature span (900-120 °C for the experiment versus 450-120 °C for sublimates from Mutnovsky volcano), and in the crystal growth rate (2-6 hours in the experiment vs. 60-120 days on the volcano). There is no doubt that the extended temperature range and the crystal growth rate are related: higher temperatures of sublimate precipitation mean higher VMS concentrations and, as a consequence, faster crystal growth.

The highest-temperature phase (900-800 °C), as was observed in the sublimates from Mutnovsky volcano [18], is pyrrhotite (FeS) (Figure 13a). At slightly lower temperatures, pyrrhotite is replaced by chalcopyrite octahedra (CuFeS<sub>2</sub>) (Figure 13b). Cuprite (Cu<sub>2</sub>O) is a mineral of isometric system, but it forms triangular crystals that appear to be flattening along the triple symmetry axis (Figure 13c, d). Further, greenockite (CdS) appears instead of Fe-Cu sulfides, which forms hexagonal prismatic crystals and aggregates of various shapes (Figures 13e, f). Galena (PbS) is often adjacent to greenockite (Figure 13f). Halite-sylvite precipitates are widespread in a significant part of all experimental tubes, with a Na:K ratio of approximately 1:1.

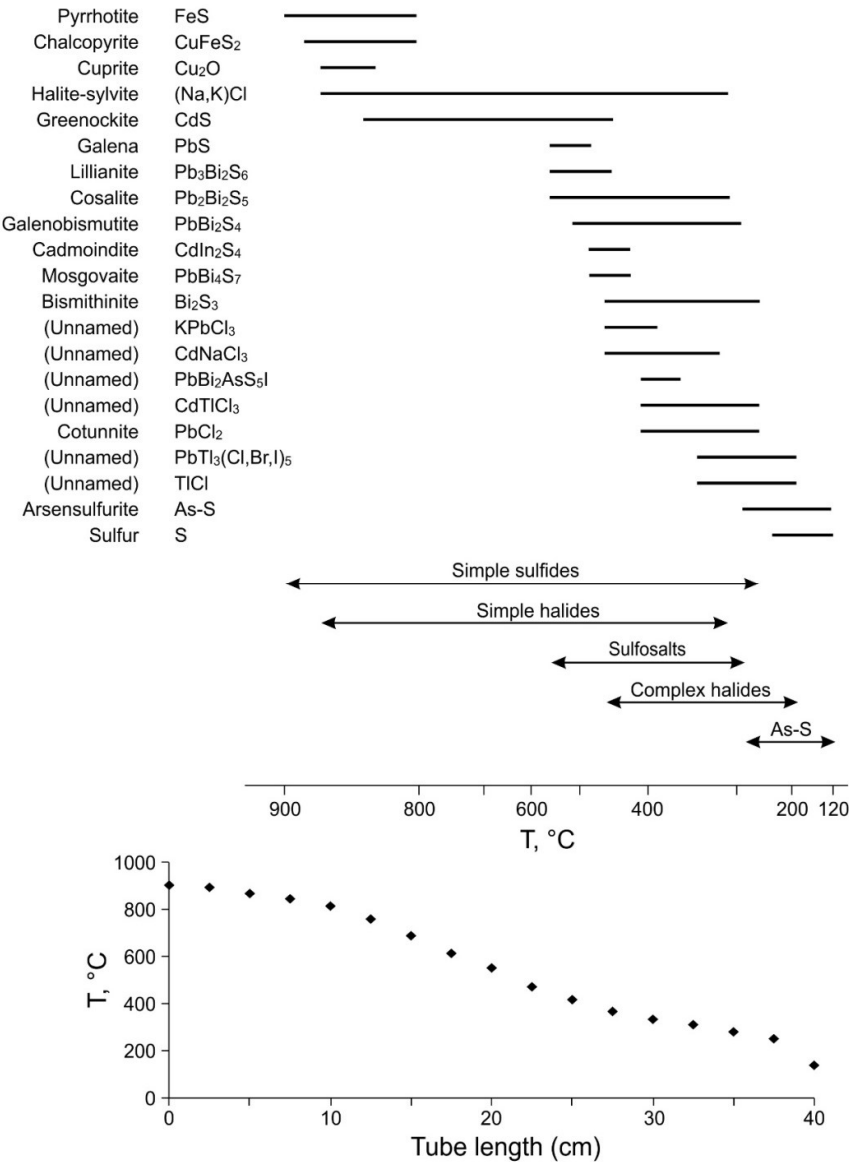


**Figure 11.** Deposition sequence of experimental sublimates in the silica glass tubes as a function of temperature (top) and measured temperature distribution along the tube (bottom). The diagram shows the average for three tubes: some tubes may have been missing certain phases. Only phases that were confidently identified are shown.

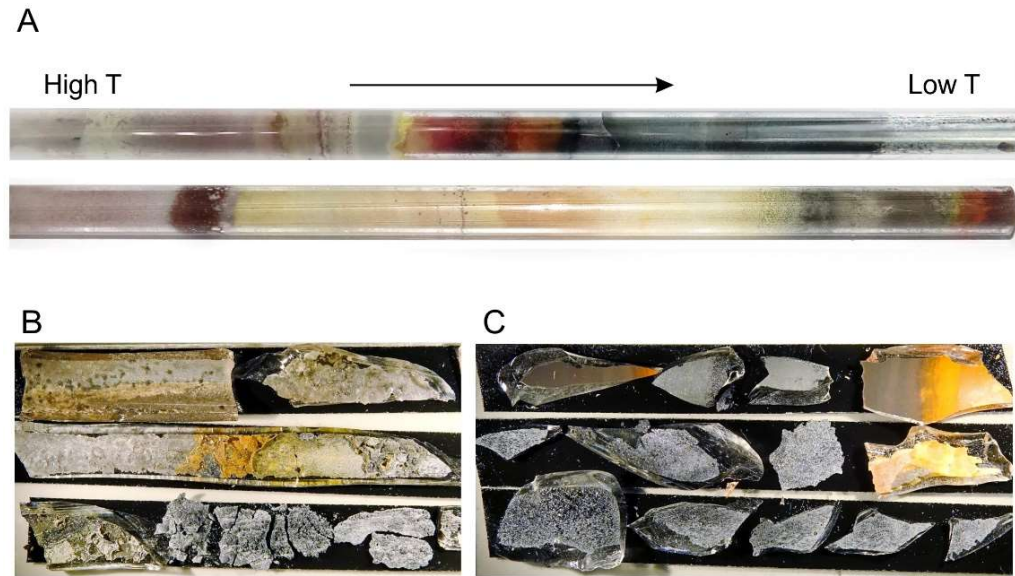


**Figure 12.** Silica glass tubes with experimental sublimates. A, Clearly visible temperature zoning in tubes coated from the inside with multi-colored sublimates. B and C, Fragments of tubes with sublimates glued to glass holders for study under a scanning electron microscope, without carbon coating. Pale deposits in B are Na-K chloride, light brown – CdS. In C, yellow and orange deposits are thallium halides, gray are sulfosalts.

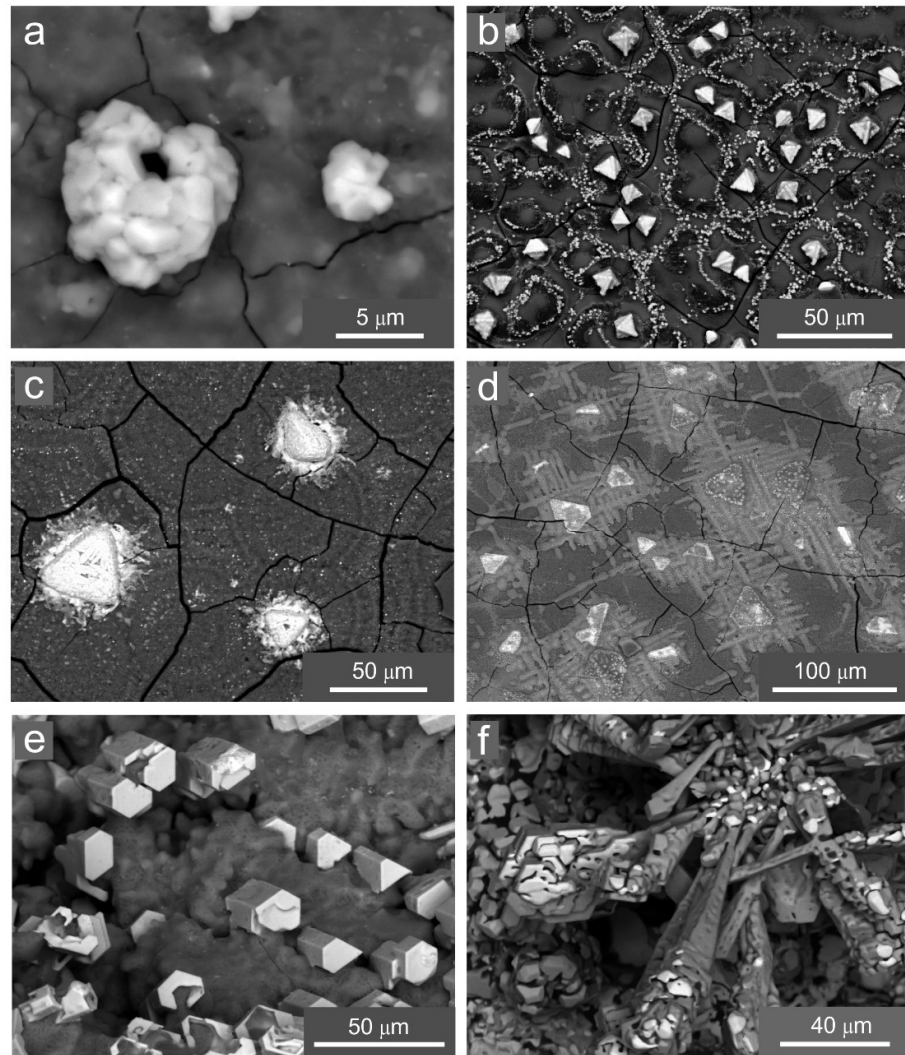


**Figure 13.** Experimental results: simple sulfides and chlorides. a, Pyrrhotite ( $\text{FeS}$ ). b, Chalcopyrite ( $\text{CuFeS}_2$ ). c, Cuprite ( $\text{Cu}_2\text{O}$ , pseudomorphs after chalcopyrite). d, Cuprite (triangles) and halite-sylvite ( $\text{NaCl-KCl}$ , lattice). e, Greenockite ( $\text{CdS}$ , hexagonal prisms) in halite-sylvite matrix. f, Aggregates of greenockite (sword-like aggregates) and galena (white crystals). Electron micrographs, back-scattered electron images.



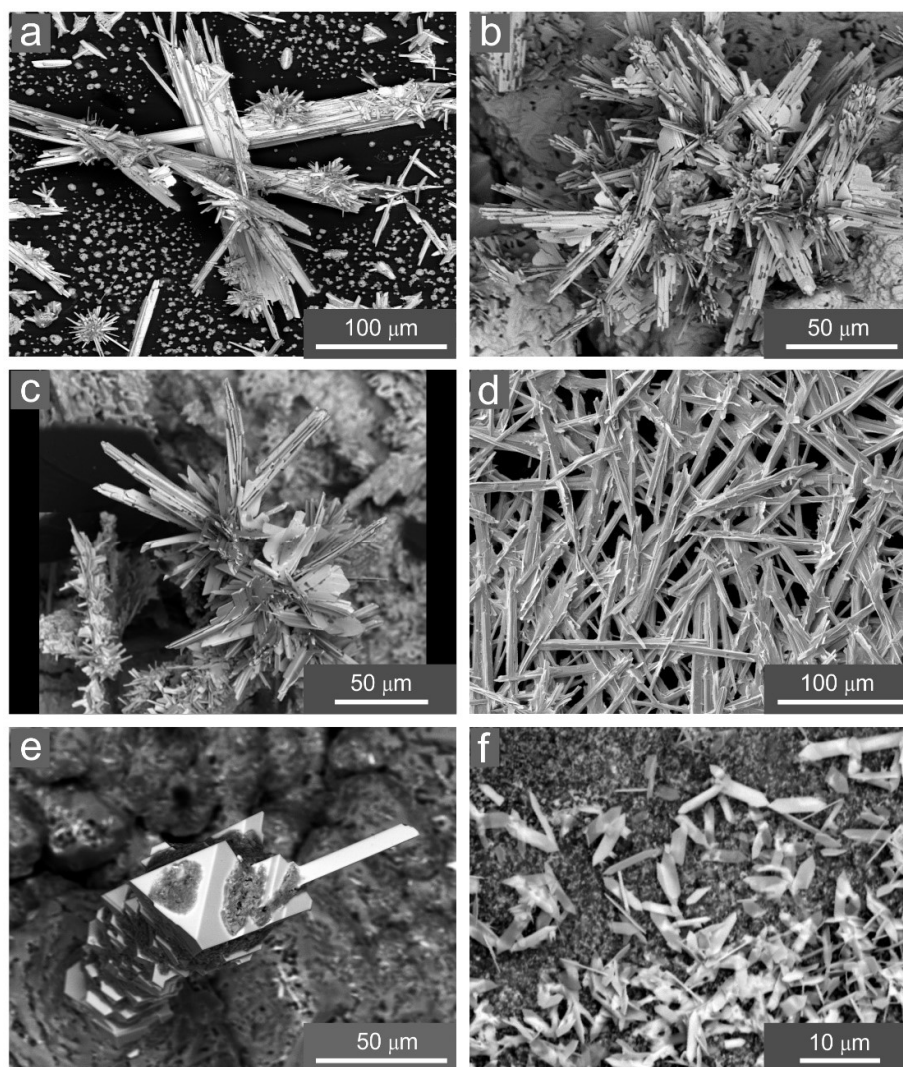


**Figure 14.** Experimental results: sulfosalt zone. a, Lillianite ( $\text{Pb}_3\text{Bi}_2\text{S}_6$ ). b, Cosalite ( $\text{Pb}_2\text{Bi}_2\text{S}_5$ ). c, Galenobismutite ( $\text{PbBi}_2\text{S}_4$ ). d, Bismutinite ( $\text{Bi}_2\text{S}_3$ ). e, Cadmoindite ( $\text{CdIn}_2\text{S}_4$ , octahedra) and mozgovaite ( $\text{PbBi}_4\text{S}_7$ , needle) in a halite-sylvite matrix (dark gray). f, Cotunnite ( $\text{PbCl}_2$ , white crystals) and halite-sylvite. Electron micrographs, back-scattered electron images.

One of the most interesting experimental results is precipitation of various lead-bismuth sulfosalts, as well as the rare mineral cadmoindite (Figure 14). Lead-bismuth sulfosalts are important ore-forming minerals and are widespread among the minerals of fumarolic fields [21] and in sublimates obtained on active volcanoes [18]. However, Pb-Bi sulfosalts have not yet been obtained in experiments on gaseous transport of metals. The rarest mineral among the synthesized sulfosalts is cadmoindite  $\text{CdIn}_2\text{S}_4$ , which has so far been described as rare finds on only two volcanoes of the Kurile Islands, namely Kudryavy volcano [46] and Ebeko volcano [47]. We determined cadmoindite by its chemical composition and very noticeable octahedron shapes of crystals. Earlier, the presence of cadmoindite in experimental deposits from the gas claimed [Renggli, C.J. and Klemme, S. \[28\]](#), but they described completely different needle-like shape of the mineral crystals.



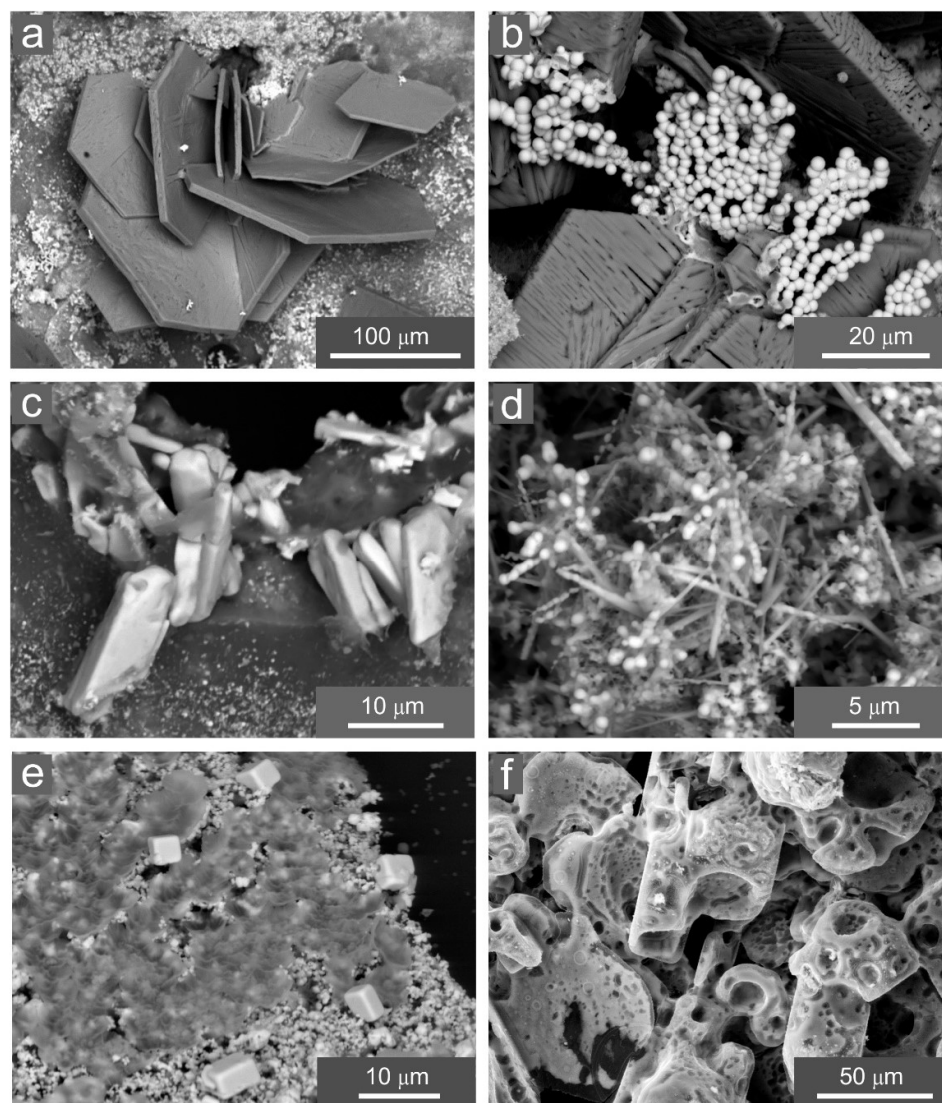


**Figure 15.** Experimental results: complex halides, arsenic and sulfur. a,  $\text{CdNaCl}_3$ , unnamed mineral. b,  $\text{PbBi}_2\text{AsS}_5\text{I}$ , unnamed mineral (white spheres) and  $\text{CdNaCl}_3$ , gray crystals. c,  $\text{CdTiCl}_3$ . d,  $\text{CdTiCl}_3 + \text{PbTl}_3$  (Cl, Br, I) 5. e, As-S (arsensulfurite, gray matrix) and thallium chloride ( $\text{TlCl}$ , cubes). f, Native sulfur. Electron micrographs, back-scattered electron images.

Halides account for an appreciable part of the experimental sublimates. Na-K chloride is the most abundant and occurs in the temperature range of 250 – 850 °C. Judging by the shape of the aggregates (Figures 12d, e) and the deposition temperature, (Na,K)Cl could condense in the high-temperature end of the tubes in the form of liquid droplets. NaCl and KCl form eutectic at a ratio of approximately 1: 1 with a solidification temperature of 657 °C. Below this temperature, (Na,K)Cl is also present but condensed from the gas directly into a solid phase. In addition to Na-K chloride, several halides containing heavy metal were found in the tubes. Of these compounds, some are quite common as natural minerals (cotunnite  $\text{PbCl}_2$ ), others are rare minerals (lafossaitite  $\text{TlCl}$ , [48]), and some compounds such as  $\text{NaCdCl}_3$  type have not yet been registered as minerals, although they have been described in volcanic aerosols [45].

More complex compounds were found closer to the low-temperature end of the tubes. For example, it was the iodine-containing sulfosalt of the composition  $\text{PbBi}_2\text{AsS}_5\text{I}$ ,

which has no analogues either among natural minerals or among artificially synthesized compounds. The phase forms micron-sized chain aggregates of spherules (Figure 15b), which are clearly visible under an electron microscope due to their specific shape and the presence of heavy elements in the composition. However, the composition of this phase is close to that of iodine-containing sulfosalt mutnovskite  $\text{Pb}_2\text{AsS}_3(\text{I}, \text{Cl}, \text{Br})$  and especially to the chlorine-containing sulfosalt tazieffite  $\text{Pb}_2\text{BiAs}_2\text{S}_5(\text{Cl}, \text{I}, \text{Br})$ . Both halide-containing sulfosalts were previously described at Mutnovsky volcano [49, 50], with tazieffite forming thin needles, and mutnovskite forming small isometric crystals.

#### 4. Discussion

##### 4.1. Comparison of low- and 1 atm-pressure “bench fumarole” experiments

Similar to silica glass tubes installed on volcanoes [25], our experiments should be considered as a method for volcanic gas study in order to better understand natural processes. The phenomenon of gaseous transport and deposition of elements on volcanoes has long been known [51, 52, and references therein]. This phenomenon is widely used in industry [e.g., 52, 53]. However, only a few attempts are known to simulate and reproduce in the laboratory the deposition of natural fumarolic minerals from the gas phase [27-31, 54]. In some works [27, 28], the transport of elements at a reduced pressure of  $\sim 10^{-5}$  bar have been studied; the rest concerned the gas-phase transport of elements and deposition of minerals at atmospheric pressure. Semenova et al [54] investigated the synthesis of some fumarolic minerals by the chemical vapor deposition method at low pressure. All the researchers listed above did not aim to accurately reproduce the composition of the fumarolic gas. This goal was firstly formulated and partially solved in the present work.

Our experiments have shown that mineral precipitates from the gas (“sublimates”) obtained at low pressure ( $10^{-5}$  bar) and in the absence of water are very similar in the mineral composition and in the crystal habits to minerals obtained from the model gas rich in water at atmospheric pressure. This is especially noticeable in comparing our “sublimates” with those demonstrated in the work by Renggli, C.J. and Klemme, S. [28], where researchers managed to obtain not only simple chlorides and sulfides, but also more complex compounds such as cadmoindite  $\text{CdIn}_2\text{S}_4$  or complex oxides like  $3\text{CdO} \cdot 2\text{TeO}_2 \cdot \text{MoO}_3$ . The most plausible explanation for this result is that the properties of a fumarolic gas are very close to the ideal gas properties, in which the molecules do not interact physically or chemically with each other. It is a well-known fact that low-density gases, for example, air, differ little in behavior from an ideal gas [e.g., 55]. Our experiments have shown that, most likely, fumarolic gases (and in particular, VMS in such gases) are close to an ideal gas, despite the fact that such gases consist of highly reactive compounds. Reactive volatile components, including  $\text{H}_2\text{O}$ ,  $\text{HCl}$ , sulfur species and other volatiles, are actually serve as an inert medium that only carries volatile metal species. Of course, a small part of the reactive compounds should necessarily react with elements (for example, with oxides in our experiment or with silicate glass/melt in the case of natural fumaroles), and as a result, VMS would be formed, which then will evaporate into the gas (the so-called volatilization, e.g., Symonds et al. [7]). But then, VMS and reactive major gas species do not interact with each other. The interaction occurs on the surface where volatile species condense and react, forming crystals.

Experiments with a flow-through reactor and with transport of elements in a reactive model gas, fully replicating the composition of natural fumarolic gases can be replaced, at least partially, by more simple approaches, performed at low pressure in evacuated ampoules [27, 28, 54], when the main volatile components of fumarolic gases ( $\text{H}_2\text{O}$ ,  $\text{HCl}$ , S, HF, etc.) are present in a minimum amount sufficient just for the volatilization of elements into VMS to occur.

#### 4.2. Composition and variability of the model gas

Experiments with a flow-through reactor and complete gas composition can be used to verify the trace element composition of fumarolic gases. In contrast to experiments with evacuated ampoules [27, 28, 54], the gas flow rate in our experiments (20-30 cm<sup>3</sup>/s at 120 °C or 15-20 mg/s) allows collection of fully-featured gas samples (Figures 6, 7), which further can be conventionally analyzed by wet chemistry or ICP-MS. Further, after measuring the metal contents in the gas, it is possible to compare these data with the observed patterns of sublimates and thus to reveal factors that may determine the precipitation of one or another mineral from the gas. In particular, we noticed in our experiments that small changes in the proportions of metal oxides in the feeding ampoule lead to significant changes in the composition of mineral precipitates at the outlet nozzle of the reactor.

Comparison of our artificially obtained sequence of sublimates (Figure 11) with natural sublimates at Mutnovsky Volcano [18] showed that both sublimate patterns are very similar, despite the different temperature ranges of mineral deposition (900 – 120 and 450 – 120 °C, respectively). With the increase of the gas temperature, VMS concentrations grow exponentially, increasing by about an order of magnitude with every 100-degree step of temperature increase [7, 23, 33]. It follows from this fact that our model gas at the maximum temperature (900 °C) can transport 3-4 orders of magnitude more elements than fumarolic gas, for example, at Mutnovsky volcano. In fact, the experimentally obtained sublimates during 2-6 hours were comparable in their mass and visual appearance to sublimates from Mutnovsky volcano, where deposition from gas lasted for 60-120 days, i.e. approximately three orders of magnitude longer. The actual concentration of metals in the model gas can be obtained by the gas sampling and analysis. However, even without this, but it is obvious even without such analyses that the deposition from the gas of one or another phase is determined not by the temperature itself, but by the saturation of the gas with respect to one or another mineral phase.

According to our observations, in the case of some proportional increase in the concentrations of all VMS in the gas, the sequence of deposited sublimates is retained, shifting to the zone of higher temperatures. Simultaneously the growth rate of sublimates increases proportionally to increase in the concentrations of elements. At least, this is true for the studied temperature range (900 – 120 °C) and compositional range of the model gases (Tables 1 and 2).

#### 5. Conclusions

A laboratory installation has been made that makes it possible to simulate the gaseous transport of elements and mineral deposition from the gas phase at atmospheric pressure. Unlike previous works, the installation closely reproduces the composition of the volcanic gas not only in terms of the main gas components (H<sub>2</sub>O, CO<sub>2</sub>, SO<sub>2</sub>, H<sub>2</sub>S, HF, HCl), but also the trace element composition (metals and metalloids) in quantities characteristic of fumarolic and volcanic gases.

In an experiment with reduced gas composition (SO<sub>2</sub>:H<sub>2</sub>S ratio = 2:1), a sequence of sublimates was obtained, which closely coincides with the sublimates observed on volcanoes. In particular, the experimental sublimates contain a characteristic sequence "simple sulfides - simple halides - complex sulfides - complex halides", which is known for natural fumarolic fields. This sequence includes five complex sulfosalts, which were previously described for natural fumaroles.

Sublimates obtained at low pressure in evacuated ampoules (10<sup>-5</sup> bar) from a gas that does not contain water vapor, and sublimates obtained at atmospheric pressure from a model gas that fully reproduces natural fumarolic gas, are very similar in their phase composition and appearance. This observation may indicate that the behavior of fumarole gases, including volatile metal species, closely matches the behavior of an ideal gas. The main factor determining the onset of desublimation of a mineral from gas is the supersaturation of the gas with respect to one or another mineral phase. The growth rate of

---

mineral precipitates from the gas phase was found to be approximately proportional to the concentrations of metals and metalloids in the gas.

**Author Contributions:** For research articles with several authors, a short paragraph specifying their individual contributions must be provided. The following statements should be used “Conceptualization, M.Z. and Yu.T.; methodology, M.Z.; investigation, M.Z., A.A.K and F.D.S; resources, M.Z.; writing—original draft preparation, M.Z. and Yu.T.; writing—review and editing, M.Z.; project administration, M.Z.; funding acquisition, M.Z. All authors have read and agreed to the published version of the manuscript.

**Funding:** This research was funded by Russian Foundation for Basic Research, grant number 19-05-00777.

**Data Availability Statement:** the study did not report any data.

**Acknowledgments:** In this section, you can acknowledge any support given which is not covered by the author contribution or funding sections. This may include administrative and technical support, or donations in kind (e.g., materials used for experiments).

**Conflicts of Interest:** Declare conflicts of interest or state “The authors declare no conflict of interest.” Authors must identify and declare any personal circumstances or interest that may be perceived as inappropriately influencing the representation or interpretation of reported research results. Any role of the funders in the design of the study; in the collection, analyses or interpretation of data; in the writing of the manuscript, or in the decision to publish the results must be declared in this section. If there is no role, please state “The funders had no role in the design of the study; in the collection, analyses, or interpretation of data; in the writing of the manuscript, or in the decision to publish the results”.

## References

1. Symonds, R.B.; Rose, W.I.; Bluth, G.J.S.; Gerlach, T.M. "Volcanic-gas studies: methods, results, and applications." In *Volatiles in Magmas*, edited by Carroll, M.R.; Holloway, J.R., 1-66. Washington, D.C.: Mineralogical Society of America, 1994.
2. Giggenbach, W.F. Chemical Composition of Volcanic Gases. *Monitoring and Mitigation of Volcano Hazards* 1996, 36.
3. Fischer, T.P.; Chiodini, G. "Chapter 45 - Volcanic, Magmatic and Hydrothermal Gases." In *The Encyclopedia of Volcanoes (Second Edition)*, edited by Sigurdsson, H., 779-97. Amsterdam: Academic Press, 2015.
4. Taran, Y.; Zelenski, M. Systematics of water isotopic composition and chlorine content in arc-volcanic gases. *Geological Society, London, Special Publications* 2015, 410, 1, 237.
5. Stoiber, R.E.; Rose, W.I. Fumarole incrustations at active central american volcanoes. *Geochim. Cosmochim. Acta* 1974, 38, 4, 495-516.
6. Africano, F.; Bernard, A. Acid alteration in the fumarolic environment of Usu volcano, Hokkaido, Japan. *J. Volcanol. Geotherm. Res.* 2000, 97, 1, 475-95.
7. Symonds, R.B.; Rose, W.I.; Reed, M.H.; Lichte, F.E.; Finnegan, D.L. Volatilization, transport and sublimation of metallic and non-metallic elements in high temperature gases at Merapi Volcano, Indonesia. *Geochim. Cosmochim. Acta* 1987, 51, 2083-101.
8. Inostroza, M.; Aguilera, F.; Menzies, A.; Layana, S.; González, C.; Ureta, G.; Sepúlveda, J.; Scheller, S.; Böhm, S.; Barraza, M.; Tagle, R.; Patzschke, M. Deposition of metals and metalloids in the fumarolic fields of Guallatiri and Lastarria volcanoes, northern Chile. *J. Volcanol. Geotherm. Res.* 2020, 393, 106803.
9. Symonds, R.B.; Reed, M.H. Calculation of multicomponent chemical equilibria in gas-solid- liquid systems: calculation methods, thermochemical data, and applications to studies of high-temperature volcanic gases with examples from Mount St. Helens. *Am. J. Sci.* 1993, 293, 8, 758-864.
10. Kavalieris, I. High Au, Ag, Mo, Pb, V and W content of fumarolic deposits at Merapi volcano, central Java, Indonesia. *J. Geochem. Explor.* 1994, 50, 1, 479-91.
11. Bernard, A.; Le Guern, F. Condensation of volatile elements in high-temperature gases of Mount St. Helens. *J. Volcanol. Geotherm. Res.* 1986, 28, 1, 91-105.
12. Zambonini, F.; Carobbi, G.; Washington, H.S. A chemical study of the yellow incrustations on the vesuvian lava of 1631. *Am. Mineral.* 1927, 12, 1, 1-10.
13. Zies, E.G. The valley of ten thousand smokes: I. The fumarolic incrustations and the bearing ore deposition., II. The acid gases contributed to the sea during volcanic activity. *National Geographic Society, Contributed Technical Papers, Katmai Series* 1929, 4, 79.
14. Papike, J.J.; Keith, T.E.C.; Spilde, M.N.; Galbreath, K.C.; Shearer, C.K.; Laul, J.C. Geochemistry and mineralogy of fumarolic deposits, Valley of Ten Thousand Smokes, Alaska: Bulk chemical and mineralogical evolution of dacite-rich protolith. *Am. Mineral.* 1991, 76, 9-10, 1662-73.
15. Krauskopf, K.B. The possible role of volatile metal compounds in ore genesis. *Econ. Geol.* 1964, 59, 1, 22-45.
16. Williams-Jones, A.E.; Heinrich, C.A. 100th Anniversary special paper: Vapor transport of metals and the formation of magmatic-hydrothermal ore deposits. *Econ. Geol.* 2005, 100, 7, 1287-312.
17. Taran, Y.A.; Bernard, A.; Gavilanes, J.C.; Lunezheva, E.; Cortés, A.; Armienta, M.A. Chemistry and mineralogy of high-temperature gas discharges from Colima volcano, Mexico. Implications for magmatic gas-atmosphere interaction. *J. Volcanol. Geotherm. Res.* 2001, 108, 1, 245-64.
18. Zelenski, M.; Bortnikova, S. Sublimate speciation at Mutnovsky volcano, Kamchatka. *Eur. J. Mineral.* 2005, 17, 1, 107-18.
19. Taran, Y.A.; Bernard, A.; Gavilanes, J.C.; Africano, F. Native gold in mineral precipitates from high-temperature volcanic gases of Colima volcano, Mexico. *Appl. Geochem.* 2000, 15, 3, 337-46.



20. Zelenski, M.; Kamenetsky, V.S.; Hedenquist, J. Gold recycling and enrichment beneath volcanoes: A case study of Tolbachik, Kamchatka. *Earth Planet. Sci. Lett.* 2016, 437, 35–46.
21. Balić-Žunić, T.; Garavelli, A.; Jakobsson, S.P.; Jonasson, K.; Katerinopoulos, A.; Kyriakopoulos, K.; Acquafredda, P. "Fumarolic Minerals: An Overview of Active European Volcanoes." In *Updates in Volcanology - From Volcano Modelling to Volcano Geology*, edited by Nemeth, K., 2016.
22. Symonds, R. Scanning electron microscope observations of sublimates from Merapi Volcano, Indonesia. *Geochem. J.* 1993, 27, 4-5, 337-50.
23. Churakov, S.V.; Tkachenko, S.I.; Korzhinskii, M.A.; Bocharnikov, R.E.; Shmulovich, K.I. Evolution of Composition of High-Temperature Fumarolic Gases from Kudryavy Volcano, Iturup, Kuril Islands: the Thermodynamic Modelling. *Geochem. Int.* 2000, 38, 5.
24. Pekov, I.V.; Agakhanov, A.A.; Zubkova, N.V.; Koshlyakova, N.N.; Shchipalkina, N.V.; Sandalov, F.D.; Yapaskurt, V.O.; Turchkova, A.G.; Sidorov, E.G. Oxidizing-Type Fumaroles of the Tolbachik Volcano, a Mineralogical and Geochemical Unique. *Russ. Geol. Geophys.* 2020, 61, 5-6, 675-88.
25. Le Guern, F.; Bernard, A. A new method for sampling and analyzing volcanic sublimates — application to Merapi volcano, Java. *J. Volcanol. Geotherm. Res.* 1982, 12, 1, 133-46.
26. Zelenski, M.E.; Fischer, T.P.; de Moor, J.M.; Marty, B.; Zimmermann, L.; Ayalew, D.; Nekrasov, A.N.; Karandashev, V.K. Trace elements in the gas emissions from the Erta Ale volcano, Afar, Ethiopia. *Chem. Geol.* 2013, 357, 95-116.
27. Nekvasil, H.; DiFrancesco, N.J.; Rogers, A.D.; Coraor, A.E.; King, P.L. Vapor-Deposited Minerals Contributed to the Martian Surface During Magmatic Degassing. *Journal of Geophysical Research: Planets* 2019, 124, 6, 1592-617.
28. Renggli, C.J.; Klemme, S. Experimental constraints on metal transport in fumarolic gases. *J. Volcanol. Geotherm. Res.* 2020, 400, 106929.
29. Scholtysik, R.; Canil, D. Investigation of the effect of Cl on the transport and sublimation of volatile trace metals in volcanic gases using benchtop fumarole experiments. *J. Volcanol. Geotherm. Res.* 2020, 395, 106838.
30. Scholtysik, R.; Canil, D. The effects of S, Cl and oxygen fugacity on the sublimation of volatile trace metals degassed from silicate melts with implications for volcanic emissions. *Geochim. Cosmochim. Acta* 2021, 301, 141-57.
31. Scholtysik, R.; Canil, D. Condensation behaviour of volatile trace metals in laboratory benchtop fumarole experiments. *Chem. Geol.* 2018, 492, 49-58.
32. Symonds, R.B.; Reed, M.H.; Rose, W.I. Origin, speciation, and fluxes of trace-element gases at Augustine volcano, Alaska: Insights in magma degassing and fumarolic processes. *Geochim. Cosmochim. Acta* 1992, 56, 633-57.
33. Wahrenberger, C.M. Some aspects of the chemistry of volcanic gases. PhD ETH Zurich, 1997.
34. Mioduszewski, L.; Kress, V. Laboratory calibration of chemical volcanic gas sampling techniques using an artificial fumarole. *J. Volcanol. Geotherm. Res.* 2008, 174, 4, 295-306.
35. Feng, T.; Huo, M.; Zhao, X.; Wang, T.; Xia, X.; Ma, C. Reduction of SO<sub>2</sub> to elemental sulfur with H<sub>2</sub> and mixed H<sub>2</sub>/CO gas in an activated carbon bed. *Chemical Engineering Research and Design* 2017, 121, 191-99.
36. Peterfreund, R.A.; Philip, J.H. Critical parameters in drug delivery by intravenous infusion. *Expert Opinion on Drug Delivery* 2013, 10, 8, 1095-108.
37. Laperdrix, E.; Justin, I.; Costentin, G.; Saur, O.; Lavalley, J.C.; Aboulayt, A.; Ray, J.L.; Nédéz, C. Comparative study of CS<sub>2</sub> hydrolysis catalyzed by alumina and titania. *Applied Catalysis B: Environmental* 1998, 17, 1, 167-73.
38. Sun, X.; Ning, P.; Tang, X.; Yi, H.; Li, K.; He, D.; Xu, X.; Huang, B.; Lai, R. Simultaneous catalytic hydrolysis of carbonyl sulfide and carbon disulfide over Al<sub>2</sub>O<sub>3</sub>-K/CAC catalyst at low temperature. *Journal of Energy Chemistry* 2014, 23, 2, 221-26.
39. Bacon, R.F.; Boe, E.S. Hydrogen Sulfide Production from Sulfur and Hydrocarbons. *Industrial & Engineering Chemistry* 1945, 37, 5, 469-74.

40. Crane, S.R.; Crocker, L.; Nissen, W.I. *Hydrogen Sulfide Generation by Reaction of Natural Gas, Sulfur, and Steam*. Vol. 8539: US Department of the Interior, Bureau of Mines, 1981.
41. Chernysheva, A.V.; Basevich, V.Y.; Vedeneev, V.I.; Arutyunov, V.S. Mechanism of gas-phase oxidation of hydrogen sulfide at high temperatures. *Bulletin of the Academy of Sciences of the USSR, Division of chemical science* 1990, 39, 9, 1775-84.
42. Giggenbach, W.F. Redox processes governing the chemistry of fumarolic gas discharges from White Island, New Zealand. *Appl. Geochem.* 1987, 2, 2, 143-61.
43. Chemical Reaction and Equilibrium Software with Thermochemical Database and Simulation Module, HSC Chemistry 6.1. Outotec Research.
44. Giggenbach, W.F. A simple method for the collection and analysis of volcanic gas samples. *Bulletin Volcanologique* 1975, 39, 1, 132-45.
45. Zelenski, M.; Kamenetsky, V.S.; Taran, Y.; Kovalskii, A.M. Mineralogy and Origin of Aerosol From an Arc Basaltic Eruption: Case Study of Tolbachik Volcano, Kamchatka. *Geochem. Geophys. Geosyst.* 2020, 21, 2, e2019GC008802.
46. Chaplygin, I.V.; Mozgova, N.N.; Bryzgalov, I.A.; Mokhov, A.V. Cadmoindite,  $\text{CdIn}_2\text{S}_4$ , a new mineral from Kudriavyy volcano, Iturup isle, Kurily islands. *Proceedings of the Russian Mineralogical Society* 2004, 133, 4, 21-27.
47. Shevko, E.P.; Bortnikova, S.B.; Abrosimova, N.A.; Kamenetsky, V.S.; Bortnikova, S.P.; Panin, G.L.; Zelenski, M. Trace Elements and Minerals in Fumarolic Sulfur: The Case of Ebeko Volcano, Kuriles. *Geofluids* 2018, 2018, 4586363.
48. Roberts, A.C.; Venance, K.E.; Seward, T.M.; Grice, J.D.; Paar, W.H. Lafossaite, a new mineral from the La Fossa crater, Vulcano, Italy. *The Mineralogical Record* 2006, 37, 165+.
49. Zelenski, M.; Garavelli, A.; Pinto, D.; Vurro, F.; Moëlo, Y.; Bindi, L.; Makovicky, E.; Bonaccorsi, E. Tazieffite,  $\text{Pb}_{20}\text{Cd}_2(\text{As,Bi})_{22}\text{S}_{50}\text{Cl}_{10}$ , a new chloro-sulfosalt from Mutnovsky volcano, Kamchatka Peninsula, Russian Federation. *Am. Mineral.* 2009, 94, 10, 1312-24.
50. Zelenski, M.; Balić-Žunić, T.I.; Bindi, L.; Garavelli, A.; Makovicky, E.; Pinto, D.; Vurro, F. First occurrence of iodine in natural sulfosalts: The case of mutnovskite,  $\text{Pb}_2\text{AsS}_3(\text{I,Cl,Br})$ , a new mineral from the Mutnovsky volcano, Kamchatka Peninsula, Russian Federation. *Am. Mineral.* 2006, 91, 1, 21-28.
51. Bunsen, R. Vulkanische exhalation. *J. Prakt. Chem.* 1852, 56, 53.
52. Binnewies, M.; Glaum, R.; Schmidt, M.; Schmidt, P. Chemical Vapor Transport Reactions – A Historical Review. *Zeitschrift für anorganische und allgemeine Chemie* 2013, 639, 2, 219-29.
53. Schaefer, H. *Chemical Transport Reactions*. New York: Academic Press, 1964.
54. Semenova, T.F.; Pankratova, O.Y.; Habanova, A.A.; R.R., S. Synthesis of exhalation copper selenites analogues by chemical gas transport reaction method (in russian). *Vestnik of St. Petersburg State University Series 4, Physics, Chemistry* 2005, 2, 75-81.
55. Lemmon, E.W.; Jacobsen, R.T.; Penoncello, S.G.; Friend, D.G. Thermodynamic Properties of Air and Mixtures of Nitrogen, Argon, and Oxygen From 60 to 2000 K at Pressures to 2000 MPa. *Journal of Physical and Chemical Reference Data* 2000, 29, 3, 331-85.